2013 IEEE/RSJ International Conference on
Intelligent Robots and Systems (IROS)
November 3-7, 2013. Tokyo, Japan

# Adaptive Internal Model Control for Mid-Ranging of Closed-Loop Systems with Internal Saturation

Olof Sörnmo, Björn Olofsson, Anders Robertsson and Rolf Johansson

*Abstract*— **This paper considers the problem of performing mid-ranging control of two closed-loop controlled systems that have internal saturations. The problem originates from previous work in machining with industrial robots, where an external compensation mechanism is used to compensate for position errors. Because of the limited workspace and the considerably higher bandwidth of the compensator, a mid-ranging control approach is proposed. An adaptive, model-based solution is presented, which is verified through simulations and experiments, where a close correspondence of the obtained results is achieved. Comparing the IAE of experiments using the proposed controller to previously established methods, a performance increase of up to 56 % is obtained.**

## I. Introduction

An experimental setup for performing high-precision milling has previously been developed and tested in milling scenarios [1], [2]. The setup consists of a conventional industrial robot and an external high-dynamic compensation mechanism [3], which is to compensate for the errors in the robot arm-side position that occur because of, *e.g.*, strong process forces and poor robot motion accuracy. However, since the external compensation mechanism only has a workspace of approximately 0.5 mm, the mechanism may reach its actuation limits when performing advanced milling tasks. Thus, we propose a mid-ranging approach for controlling the relative position between the robot and the milling tool held by the compensation mechanism.

Mid-ranging is a control strategy that is designed for the case when two actuator systems control the same variable, such as flow or position, and one of the systems is faster and possibly more accurate, but has a limited working range. The idea is then to utilize both systems to control the desired variable, making use of the higher bandwidth of the fast system, while keeping its position close to the midpoint of its working range, so as not to reach the limits [4].

In order to achieve a system that is robust to process parameter variations, which may occur because of the strong process forces of the milling process and varying cutting conditions, it is desirable to employ an adaptive control structure. However, in the scenario considered in this paper, the two actuators are already closed-loop systems which contain internal input saturations. This does not render the design of an adaptive mid-ranging controller straightforward. Motivated by this, an adaptive internal model control scheme for mid-ranging control is presented in this paper, with adaptive dynamic reference governors for handling of internal saturations, making the control approach possible.

The utilization of a robot in combination with an additional manipulator in a closed kinematic chain was investigated in [5], where the concepts of macro and micro manipulator were introduced to describe the robot and the additional compensation mechanism, respectively. The terms macro and micro manipulator are adopted in this paper.

A set of different mid-ranging control strategies were evaluated in [4], based on, *e.g.*, Valve Position Control (VPC) and Model Predictive Control (MPC). Design and tuning guidelines of VPC and Modified VPC (MVPC) controllers were presented in [6]. Anti-windup schemes for VPC controllers were introduced in [7].

Internal Model Control (IMC) was reviewed and compared with similar control strategies in [8], where also several IMC stability theorems were proven and practical tuning guidelines were provided. The problem of having a control signal saturation for an IMC controller was considered in [9]. Design and stability analysis of Adaptive Internal Model Control (AIMC) was presented in [10], and the discrete-time counterpart was described in [11]. Nonlinear approaches to AIMC were investigated in [12], as well as in [13], where neural networks were utilized.

The application of mid-ranging control using IMC was investigated in [14], where design rules were presented and verified through simulation studies.

Discrete-time Dynamic Reference Governors (DRG) for constrained nonlinear systems were considered in [15], and reference governors for systems with input and state saturations were presented in [16].

The method presented in this paper is based on [14], which is here extended by introducing adaptivity to the IMC mid-ranging structure, inspired by [10] and [11]. Further, the control scheme is modified to account for internal saturations, by introducing a dynamic reference governor based on the concepts of [16], but derived using a different approach. Further, in order to maintain good performance under parameter variation, the DRG is also made adaptive.

## II. Method

Consider two stable, discrete-time closed-loop systems on the standard feedback form, see Fig. 1, denoted $H_{cl}^{f}(z)$ and $H_{cl}^{s}(z)$, representing the micro and macro manipulator, respectively. Consequently, the bandwidth of $H_{cl}^{f}(z)$ is

O. Sörnmo, B. Olofsson, A. Robertsson, and R. Johansson are with the Department of Automatic Control, LTH, Lund University, SE–221 00 Lund, Sweden. E–mail: Olof.Sornmo@control.lth.se.

The research leading to these results has received funding from the European Union's seventh framework program (FP7/2007-2013) under grant agreement COMET (Ref. #258769) and SMErobotics (Ref. #287787). The authors are members of the LCCC Linnaeus Center and the ELLIIT Excellence Center at Lund University.

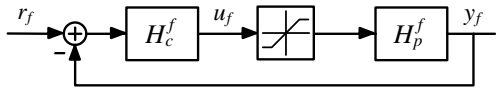


Fig. 1. Block diagram for the standard feedback form, with saturation on the input to the process. In this figure, $H_{cl}^f(z)$ is displayed.

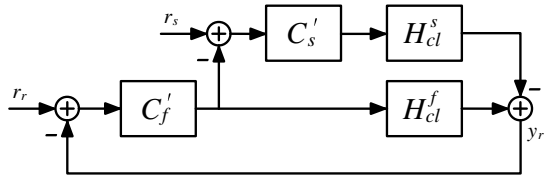


Fig. 2. Block diagram for the VPC and MVPC mid-ranging control structures.

significantly higher than that of $H_{cl}^s(z)$. The controllers in the closed-loop systems are assumed known, and the output signals of the closed-loop systems, denoted $y_f$ and $y_s$, are measured. The midpoint of the micro manipulator workspace is zero. The objective to perform mid-ranging control of the two closed-loop systems can be met by standard methods such as VPC control, as described in [4] and [6]. The block diagram for the VPC scheme is constructed as displayed in Fig. 2, where $y_r$ is the relative position of the manipulators, $r_r$ the desired relative position, and $r_s$ the desired setpoint of the mid-ranged input. It is to be noted that in this paper, since the midpoint of the micro manipulator is zero, the input $r_s$ is also zero and will hence be disregarded. The structure of the controllers $C_f'(z)$ and $C_s'(z)$ can be chosen arbitrarily, but are commonly selected as PI controllers. Experimental tuning of the controllers is tedious work and even with accurate models of the processes, arbitrary pole placement is not always possible. Internal Model Control is an appealing solution which has been proven to yield satisfactory results in mid-ranging scenarios [14]. However, as mentioned earlier, the process parameters may change over time and it is therefore desirable to adapt the IMC controller in order to correct for the process changes. The block diagram for the mid-ranging IMC is displayed in Fig. 3, where $C_f$ and $C_s$ are the controllers, $\hat{H}_{cl}^f$ and $\hat{H}_{cl}^s$ the internal models of $H_{cl}^f$ and $H_{cl}^s$, respectively. It is to be noted that the notation $C_f$ and $C_s$ represent $Q_1$ and $Q_2$, respectively, in the Youla parametrization of the IMC according to [14]. The

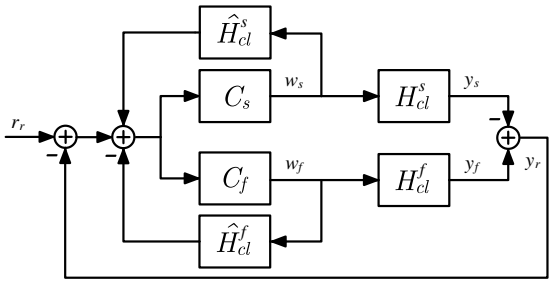


Fig. 3. Block diagram for the IMC mid-ranging control structure.

complementary sensitivity function $T_f(z)$ is introduced as the desired response of the system from $r_r$ to $y_r$, and $T_s(z)$ is the desired response of the system from $r_r$ to $y_r$ with no input to $H_{cl}^f$. In order to achieve the desired mid-ranging effect, the following conditions for the controllers must be fulfilled:

$$T_f(z) = C_f(z)H_{cl}^f(z) - C_s(z)H_{cl}^s(z) \quad (1)$$

$$T_s(z) = C_s(z)H_{cl}^s(z). \quad (2)$$

The controllers are thus calculated as

$$C_f(z) = \frac{T_f(z) + T_s(z)}{H_{cl}^f(z)} \quad (3)$$

$$C_s(z) = \frac{T_s(z)}{H_{cl}^s(z)} \quad (4)$$

where the parameters of $H_{cl}^f(z)$ and $H_{cl}^s(z)$ should be updated in order to adapt the controllers. To this purpose, a Recursive Least Squares (RLS) algorithm [17] with forgetting factor $\lambda < 1$ is introduced, because of its fast convergence for input signals of proper excitation, which is assumed to be present. For systems with low excitation, a Kalman filter might exhibit better performance. The proposed method can easily be modified to the utilization of a different estimator. The estimator is used to continuously estimate the process parameters of $H_{cl}^f$ and $H_{cl}^s$, and update the internal models $\hat{H}_{cl}^f$ and $\hat{H}_{cl}^s$, as well as the controllers $C_f$ and $C_s$.

However, as displayed in Fig 1, $H_{cl}^f$ contains an internal saturation of the inner control signal $u_f$ (denoted $u_{f,k}$ in this section, where $k$ is current sample), with a given saturation level at $\pm u_{\text{sat}}$. The system $H_{cl}^s$ is assumed not to have an internal saturation. Once the control signal saturates, *i.e.*, when the system leaves its linear region, the linear internal model can no longer accurately describe the process. Further, the estimation of $H_{cl}^f$ will be corrupted as a result of the saturation, since the input/output relation of the plant is no longer linear. This will lead to a false estimate of the system parameters and in turn unexpected behavior, in the worst case instability. This problem may be solved by implementing a nonlinear model and applying nonlinear estimation techniques, which will become intricate, especially if $H_{cl}^f$ is implemented with anti-windup. Instead, a DRG is introduced to modify the input to the system, so that the system is never allowed to enter saturation. This approach makes linear modeling still feasible. The dynamics of anti-windup schemes possibly implemented in the closed-loop system can be disregarded, since the system is designed to never enter saturation.

Consider the control structure of $H_{cl}^f$ as displayed in Fig. 1, where the controller and process dynamics are given by the rational, discrete-time transfer functions

$$H_c^f(z) = \frac{l_0 + l_1 z^{-1} + \cdots + l_{a-1} z^{-(a-1)} + l_a z^{-a}}{n_0 + n_1 z^{-1} + \cdots + n_{b-1} z^{-(b-1)} + n_b z^{-b}} \quad (5)$$

$$H_p^f(z) = \frac{q_0 + q_1 z^{-1} + \cdots + q_{c-1} z^{-(c-1)} + q_c z^{-c}}{p_0 + p_1 z^{-1} + \cdots + p_{d-1} z^{-(d-1)} + p_d z^{-d}} \quad (6)$$

where $[a, b, c, d] \in Z_0$. The objective of the DRG is to dynamically modify the reference input $r_{f,k}$ to $H_{cl}^f$, so that $|u_{f,k}| \leq u_{\text{sat}}, \forall k$. Since $y_{f,k}$ is assumed to be measured and $H_c^f(z)$ is known, this can be solved by simply calculating the current control signal $u_{f,k}$ and modifying the input to $H_{cl}^f$ accordingly. However, since the mid-ranging controller is meant to control an existing closed-loop system, the output of $H_{cl}^f$ may be delayed from the network connection between the controllers. Therefore, a model-based solution is proposed, that is independent of measurements of $y_{f,k}$.

The modified input to the system is denoted $w_{f,k}$, and the dynamic relation between $w_{f,k}$ and $r_{f,k}$ is given by

$$w_{f,k} = w_{f,k-1} + \alpha_k(r_{f,k} - w_{f,k-1}), \tag{7}$$

which is a first order low-pass filter with a time-varying parameter $\alpha_k$. When $\alpha_k = 1$, the filter does not affect the input and $w_{f,k} = r_{f,k}$ holds true, and conversely when $\alpha_k = 0$, $w_{f,k} = w_{f,k-1}$. Obviously, it is required that the inner process $H_p^f(z)$ contains at least one integrator, in order for the system to be able to reach any desired set-point.

When $|u_{f,k}| \leq u_{\text{sat}}, \forall k$, is satisfied, the control signal $u_{f,k}$ is given by

$$u_{f,k} = \frac{H_c^f}{1 + H_c^f H_p^f} w_{f,k} = \frac{\sum_{i=0}^{e} q_i' z^{-i}}{\sum_{i=0}^{f} p_i' z^{-i}} w_{f,k} \tag{8}$$

where $e = a + d$ and $f = \max(d + b, a + c)$. In order to determine $\alpha_k$, the predicted control signal with unaltered reference is denoted by $\hat{u}_{f,k}$ and defined as

$$\hat{u}_{f,k} = u_{f,k}|_{\alpha_k = 1}.$$

If $|\hat{u}_{f,k}| \leq u_{\text{sat}}$, there is no need to alter the input, and thus $\alpha_k = 1$. Otherwise, the desired control signal should be as large as possible, *i.e.*, $\pm u_{\text{sat}}$. The desired control signal in the current time-step $k$ is denoted $u_{f,k}^d$ and defined as

$$u_{f,k}^d = \text{sgn}(\hat{u}_{f,k}) u_{\text{sat}}$$

which together with (7) and (8) gives the expression for $\alpha_k$:

$$\alpha_k = \begin{cases} \frac{p_0' u_{f,k}^d + \chi(u_{f,k}, w_{f,k})}{q_0'(r_{f,k} - w_{f,k-1})}, & |\hat{u}_{f,k}| > u_{\text{sat}} \\ 1, & |\hat{u}_{f,k}| \leq u_{\text{sat}} \end{cases} \tag{9}$$

where

$$\chi(u_{f,k}, w_{f,k}) = \sum_{i=1}^{f} p_i' z^{-i} u_{f,k} - \sum_{i=1}^{e} q_i' z^{-i} w_{f,k} - q_0' w_{f,k-1} \tag{10}$$

It is clear from (9) that $q_0' \neq 0$ must be fulfilled, *i.e.*, that $H_c^f(z)$ must have a direct feedthrough path, which can easily be satisfied by a proportional part in the controller.

Since the system $H_{cl}^f(z)$ is likely to be time-varying, and the inner controller $H_c^f(z)$ is fixed, the inner process $H_p^f(z)$ must be estimated in order to adapt the DRG to the process changes. Since measurements of $u_{f,k}$ are not available, and it is only estimated based on time-invariant models, the process dynamics $H_p^f(z)$ cannot be determined based on the estimations. However, under the assumption that $|u_{f,k}| \leq u_{\text{sat}}, \forall k$, holds true, the inner process of the system can be expressed in terms of $H_{cl}^f(z)$, which is already estimated to adapt the IMC controller, and $H_c^f(z)$;

$$H_p^f(z) = \frac{H_{cl}^f(z)}{H_c^f(z)(1 - H_{cl}^f(z))}. \tag{11}$$

Since $H_c^f(z)$ is known, past measured values of $y_f$ can be used to calculate the real values of past control signals, in order to improve the prediction of $u_{f,k}$, reducing errors that occur because of process variation.

Before activating the AIMC controller, an initial estimation phase is performed, using a square wave as input to the systems, until the estimated models have reached the desired accuracy. During this phase, the requirement $|u_{f,k}| \leq u_{\text{sat}}, \forall k$, is unlikely to be fulfilled by the DRG since its prediction model is being estimated. Therefore it is important to choose the excitation signal such that the system does not saturate during this phase.

The final control architecture for the mid-ranging adaptive internal model control with compensation for internal saturation is displayed in Fig. 4. Analogously, it is to be noted that the proposed approach can be extended to systems where internal saturations appear in both $H_{cl}^f$ and $H_{cl}^s$.

In order to evaluate the proposed control scheme, a comparison to existing methods, such as the MVPC structure, is performed. Following the tuning rules given in [6], the controllers $C_f$ and $C_s$ in Fig. 2, are chosen as PI controllers, and designed using the same desired closed-loop system as for the proposed controller. Since $H_{cl}^f$ contains an internal saturation, and the current control signal is not available, the PI controllers will undoubtedly suffer from integrator windup problems. However, assuming that the current control signal is available to the controller, a tracking anti-windup algorithm [7] can be implemented. Both controllers, with and without anti-windup, denoted MVPC and MVPC+AW, are evaluated in simulation and experiments.

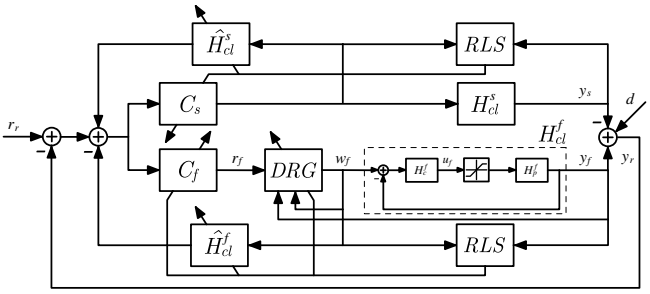


Fig. 4. Block-diagram for the mid-ranging adaptive internal model control, with internal saturation compensation.

## III. Simulation results

The proposed control scheme in Fig. 4 was implemented and tested in MATLAB Simulink, using $u_{\text{sat}} = 10$ and the

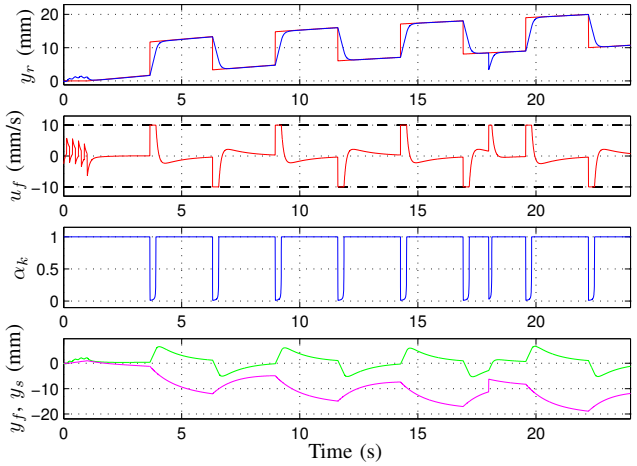


Fig. 5. Simulation result of the AIMC controller subject to a ramped square wave with a low-frequency sine wave superimposed as reference position (red curve in top plot). The relative position response is displayed in blue in the top panel, and the actuator positions in the bottom panel, where $y_f$ is green and $y_s$ is magenta. At time 18 s, the system is affected by a step position disturbance with an amplitude of 5 mm.

following systems:

$$H_c^f(z) = 5, \quad H_p^f(z) = \frac{2hz^{-1}}{1-z^{-1}}, \quad H_{cl}^s(z) = \frac{1-e^{-h}}{1-e^{-h}z^{-1}}$$

where $h$ is the sample time of the simulation, in this case $h = 0.004$ s. The desired complementary sensitivity functions are set to

$$T_f(z) = H_{cl}^f(z), \quad T_s(z) = H_{cl}^s(z) \tag{12}$$

which corresponds to preserving the bandwidths of the closed-loop systems. This choice is motivated by the assumption that the systems are well-controlled closed-loop systems, ideally having as high bandwidth as possible. An initial guess is provided to the estimators, and the systems are excited using a low amplitude square wave. In the first simulation, a ramped square wave with a superimposed low frequency sine wave is sent as relative position reference $r_r$ and the relative position $y_r$ is subject to a step position disturbance $d$. The result of the simulation is displayed in Fig. 5. The ramped input is used to demonstrate the mid-ranging effect of the micro manipulator system position $y_f$, which is clearly visible from the bottom panel in Fig. 5, where the green curve is kept close to its midpoint. Further, it can be concluded that $H_{cl}^f$ never enters saturation, since the control signal $u_f$, which is the unsaturated control signal, is kept within the saturation bounds. It is also noted that the position disturbance at 18 s is attenuated rapidly, similar to the response of the closed-loop system. This is expected since the disturbance $d$ on $y_r$ can be seen as a disturbance on $r_r$, thus exhibiting the same dynamics as the closed-loop system from $r_r$ to $y_r$.

The second simulation focuses on testing the adaptivity of the control, *i.e.*, its robustness to process variations. The simulation is performed using the same input signal as the first simulation but without the ramp, and also increasing the gain of the plant $H_p^f(z)$ by 50 % at time 8 s, and

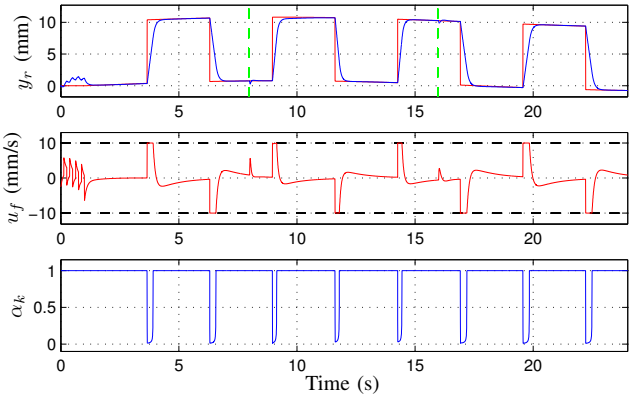


Fig. 6. Simulation result of the AIMC controller subject to a square wave with a sine wave superimposed as reference position (red curve in top plot). The relative position response is displayed in blue in the top panel. The dashed green lines indicate changes of process gain.

subsequently decreasing the gain by 60 % at time 16 s. The result of the simulation is displayed in Fig. 6. It is noted that the gain changes are only visible in the response of the relative position for one period of the square wave. Further, since the gain of $H_p^f(z)$ increases, the system becomes faster and consequently lower control signal is needed to achieve the desired response. This leads to less time in saturation and a higher value of $\alpha_k$.

The simulation results for the MVPC controllers compared to the proposed controller are presented together with the experimental results in Section V, for cohesiveness.

## IV. Experimental setup

The experimental setup used to evaluate the proposed control scheme is designed to be a small scale version meant to emulate the setup described in [1]. The setup consists of an ABB IRB2400 robot with an S4CPlus controller, which acts as the macro manipulator, and an ABB IRB120 robot with an IRC5 controller, which corresponds to the micro manipulator with high bandwidth. Naturally, both robots have saturation limits on velocity, but for proof of concept, the micro manipulator is set to have an input saturation at $\pm 80$ mm/s, and the macro manipulator is assumed to be slow enough to not reach the velocity saturation limits. In addition to the position measurements provided by the robot joint resolvers, the IRB120 robot is equipped with a Heidenhain linear encoder of model ST3078 [18], which measures the relative distance between the two robots end-effectors, with a working range of 26 mm at an accuracy of 2 µm. This measurement is essential in order to be able to compensate for arm-side position disturbances, that the motor-side robot joint resolvers are unable to measure. The IRB2400 robot is attached rigidly to the ground, while the IRB120 robot is attached to a base that can move in one direction, in order to introduce disturbances in the position, which frequently appear in the real milling setup.

The robots are interfaced using an open robot control extension of the conventional robot controller called *ORCA* [19], running at 250 Hz. MATLAB Simulink models are translated to *C*-code using *Real-Time Workshop* and

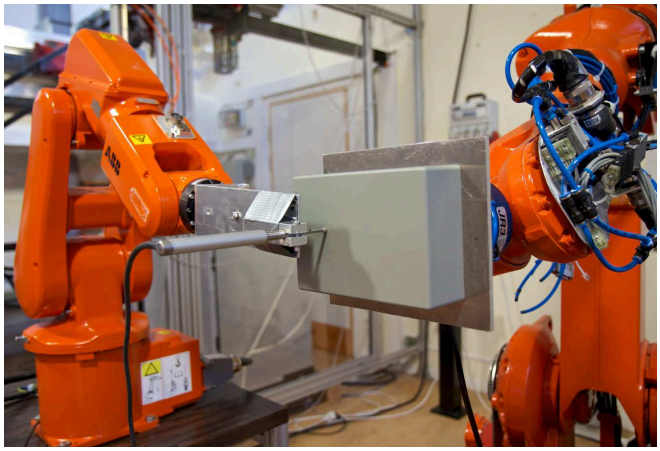

Fig. 7. Experimental setup for performing mid-ranging control. The IRB120 robot (micro manipulator) holding the Heidenhain linear encoder is seen to the left, and the IRB2400 robot (macro manipulator) to the right.

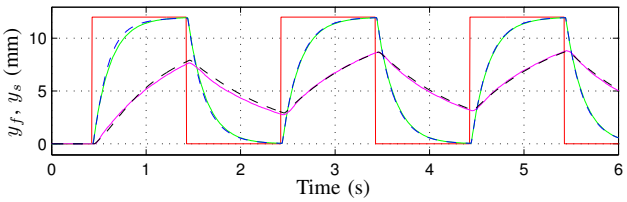


Fig. 8. Estimation phase of the two systems, where $y_f$ is green and $y_s$ magenta. The estimates of these signals are denoted $\hat{y}_f$ and $\hat{y}_s$, and are shown in dashed blue and black, respectively.

compiled in order to run them on the robot system. A picture of the experimental setup is shown in Fig. 7.

## V. Experimental Results

Prior to performing experiments, dynamic models of the two robots, with Cartesian velocity reference as input and Cartesian position as output, were identified in one axis using the Prediction Error Method [17]. In order to provide excitation for the identification algorithm, a square wave was used as reference, which is converted to joint motor angle velocity references, using the inverse Jacobian of the robot. The resulting measured Cartesian position of the robot was calculated using forward kinematics, and used as system output. Both robots exhibit similar dynamics, and the control loops that form $H_{cl}^f$ and $H_{cl}^s$, were closed using proportional controllers such that the micro manipulator system had five times higher bandwidth than the macro manipulator system. New models of the closed-loop systems were calculated, resulting in third-order models, which were used as initial guesses in the RLS estimators. The online estimation of the models was evaluated before initiating the full AIMC control structure, by sending square waves as position references to the two robots. The results of the estimation procedure is displayed in Fig. 8, where the bandwidth difference of the two systems is clearly illustrated. The desired complementary sensitivity functions $T_f$ and $T_s$ were chosen as first-order systems with bandwidths matching $H_{cl}^f$ and $H_{cl}^s$, respectively.

The first experiment performed was designed to resemble the simulation in Fig. 5, but since the linear encoder has

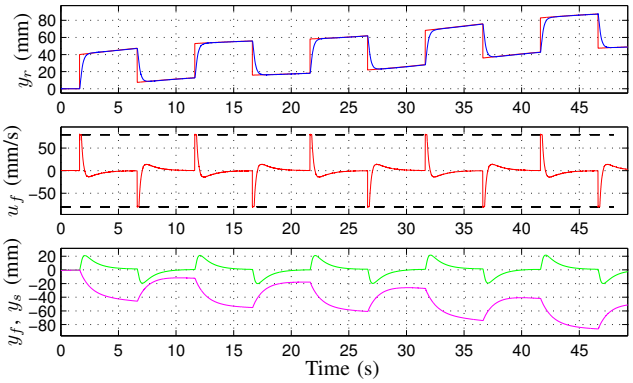


Fig. 9. Experimental result of the AIMC controller subject to a ramped square wave with a sine wave superimposed as reference position (red curve in top plot). The relative position $y_r$ response is displayed in blue in the top panel, and the robot positions in the bottom panel, where $y_f$ is green and $y_s$ is magenta.

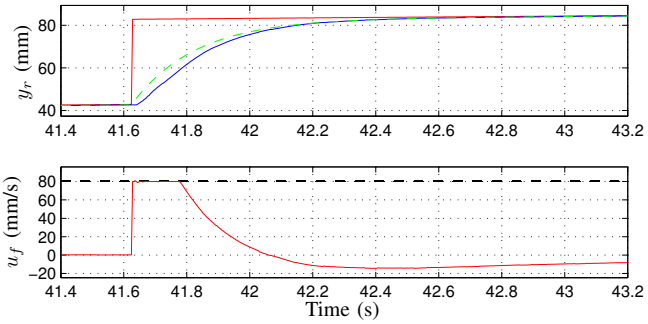


Fig. 10. Zoomed view of the step after 40 s in Fig. 9. The dashed green line shows the desired response of the system, *i.e.*, the response of $T_f(z)$.

limited measuring range, a ramp signal as input would leave that range quickly. Thus, the relative position of the robots was instead calculated from the motor-side position measurements of the robots, so that a ramp signal could be used as input. The obtained result is displayed in Fig. 9. It is evident from the figure that the desired mid-ranging effect is achieved, as well as that the control signal $u_f$ is kept within the given boundaries. A zoomed view of a step response from Fig. 9 is displayed in Fig. 10, where the desired response is also shown. It is noted that the response for the relative position $y_r$ is close to the desired response. There is however an initial discrepancy, which appears because of the fact that the fast system has an input saturation. As displayed in the lower panel of Fig. 10, the upper boundary on the control signal $u_f$ has been reached, limiting the achievable bandwidth of the closed-loop system. It is to be noted that, given a perfect model of the system, the response of the system with and without the DRG for any input signal, would look the same. The control signal before the saturation, *i.e.*, $u_f$, would however, not be the same.

Additional experiments were performed in order to test how well the system handles position disturbances. For this purpose, the linear encoder was put into operation, replacing the resolver measurements for the relative position, so that disturbances in position can be measured and compensated for. The experiment was designed such that once the esti-

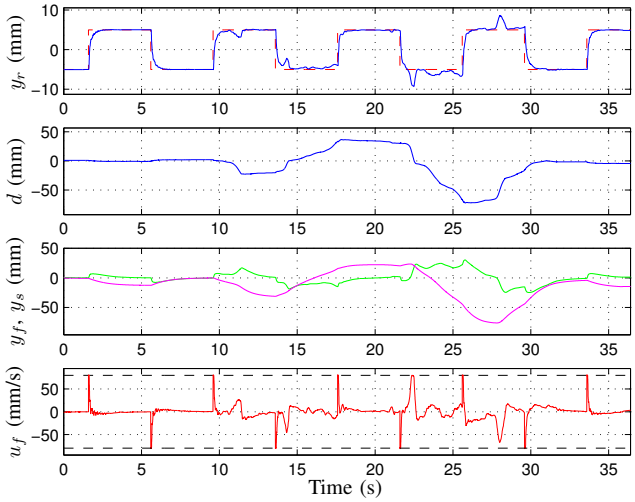


Fig. 11. Experimental result of the AIMC controller with a square wave as reference position (red curve in top plot), subject to position disturbances $d$ as displayed in the second panel. The relative position $y_r$ response is displayed in blue in the top panel, and the robot positions in the third panel, where $y_f$ is green and $y_s$ is magenta.

mation phase finishes, the macro manipulator is controlled to move until the linear encoder is in the middle of its measurement range, which is set to be the zero position. The AIMC controller is then activated, with a square wave as reference signal, while simultaneously moving the base with the micro manipulator, in order to introduce position disturbances. As mentioned earlier, the linear encoder only has a measurement range of 26 mm, and thus the amplitude of the relative position reference $r_r$ was chosen to be 5 mm. Since a smaller amplitude of the reference results in lower control signal, the desired bandwidth of $T_f$ could be increased by a factor of 5. The results of the experiment are shown in Fig. 11. It is noted that under no disturbances, the system responds rapidly in a well-damped manner. When subject to continuous disturbances, the macro manipulator has to deviate further from its desired position, in order to cancel the disturbance. It does, however, eventually return to its midpoint.

In order to evaluate the performance of the proposed control scheme, the average Integrated Absolute Error (IAE) over several step responses was chosen to quantify the performance for the different controllers. The discrete-time approximation of the IAE is defined as

$$\text{IAE} = h \sum_{k=0}^{k_{\max}} |r_{r,k} - y_{r,k}|. \tag{13}$$

The MVPC controllers were tuned as described in Sec. II, using model-order reduced versions of the previously identified models of $H_{cl}^f$ and $H_{cl}^s$. The results of a series of simulations and experiments are presented in Table I, where the IAE values have been normalized by the AIMC controller IAE value, in order to simplify comparison. The first setup was designed such that $r_r$ is small enough to fulfill $|u_f| \leq u_{\text{sat}}$, whereas the following four setups were designed for the

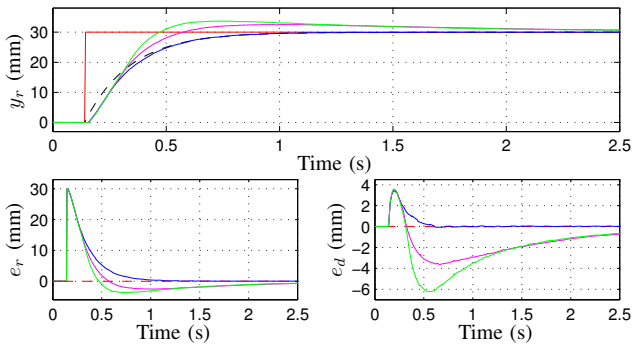


Fig. 12. Experimental step responses with $r_r = 30$, where the AIMC, MVPC+AW, and MVPC controllers are shown in blue, magenta, and green, respectively. The desired step response is shown in dashed black.

TABLE I

NORMALIZED IAE VALUE OF STEP RESPONSES.

| **Setup** | AIMC | MVPC+AW | MVPC |
|---|---|---|---|
| 1. Sim, $r_r = 1.5$ | 1.000 | 1.525 | 1.525 |
| 2. Sim, $r_r = 5$ | 1.000 | 1.458 | 1.555 |
| 3. Sim, $r_r = 5$, noise | 1.000 | 1.380 | 1.474 |
| 4. Exp, $r_r = 20$ | 1.000 | 1.344 | 1.353 |
| 5. Exp, $r_r = 30$ | 1.000 | 1.408 | 1.560 |

opposite. In the third setup, measurement noise was added in the simulation. Experiments to test the robustness to process variations were performed by attaching a weight to the micro manipulator while running the controller. Even though the weight was close to the maximum payload of the robot, however, no significant change in the process dynamics was observed. Instead, an artificial process variation was introduced by changing the gain of the input to $H_{cl}^f$. In a similar manner to the simulation studies, the gain was increased by 25 % and subsequently decreased by 30 %. The results of the experiment are shown in Fig. 13. It is evident from the figure that the performance is deteriorated once the process changes, but in approximately three periods of the input signal, the system adapted and the desired response was achieved. It is also noted that the DRG was effective in keeping the constraints, even though considerable model errors occur during the adaptation to the process change.

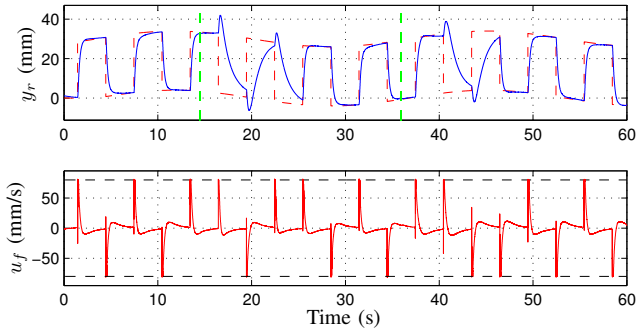


Fig. 13. Experimental result of the AIMC controller subject to a ramped square wave with a sine wave superimposed as reference position (red curve in top plot). The relative position $y_r$ response is displayed in blue in the top panel. The dashed green lines indicate changes of process gain.

## VI. Discussion and Conclusions

It was shown in simulations and verified through experiments that the proposed mid-ranging control structure for a macro and micro manipulator setup, performs satisfactory with a response close to the specification, while maintaining desired properties in the presence of internal saturations, process variations, and position disturbances. It is also noted that the obtained results from the simulations and experiments exhibit close correspondence. As shown in Table I, the performance using the proposed controller compared to the MVPC controllers in the case of time-invariant processes, is increased by as much as 56 %. In the cases where process variations are present, the proposed controller will naturally perform significantly better than the MVPC controllers, due to its adaptive properties. Furthermore, looking at the error between the system response and the desired response, the achieved IAE was up to a factor 16 lower than that of the MVPC controller, as is clearly displayed in Fig. 12. The performance of the MVPC controller depends on whether it is possible to implement anti-windup schemes, but according to the original problem formulation in this paper, it would not be possible. The MVPC controller without anti-windup will naturally perform worse for high-amplitude steps and high-frequency references, since the controller will be saturated more frequently. It could be possible to implement a DRG for the MVPC control scheme, similar to the proposed control scheme, in order to estimate the control signal for the anti-windup scheme. Since the purpose was to compare the proposed control to previously established methods, this is not considered. Further, it is noted that the performance of the proposed control scheme is deteriorated when subject to substantial measurement noise, since it corrupts the estimation of the models. This can be improved by increasing the forgetting factor to a value closer to 1, but will consequently result in slower adaptation to process variations. The proposed controller does, however, still perform 38 %–47 % better than the compared controllers. When process variations were introduced, the system adapts quickly to the new parameters, and the effects of the change can only be seen for a few periods of the input signal. It is, however, noted that the experimental results exhibit slightly slower adaptation with more pronounced transients than in simulation. This is caused by the fact that noise is present in the experiments, and as discussed earlier, the forgetting factor should be set to a higher value in order to reduce noise sensitivity. Additionally, transients appear because of the increased complexity in estimating the parameters for a third-order model, as compared to the first-order models that are used in simulation. The adaptation of the system is dependent on the excitation of the input signal, with an input signal of high degree of excitation, the system will adapt faster. Conversely, if the input signal is of low excitation, the system will adapt slowly and the transient performance will be poor. The proposed adaptive DRG was proven to be effective, as seen in Figs. 6, 10, and 13, the control signal is kept within the constraints, even under significant process variations. Even if no variations in the process dynamics are present, the adaptivity of the controller is still beneficial. This was demonstrated in Fig. 8, where it is noted that the identified models are improved throughout the estimation procedure, thus increasing the performance of the closed-loop system.

## References


[1] B. Olofsson, O. Sörnmo, U. Schneider, A. Robertsson, A. Puzik, and R. Johansson, "Modeling and control of a piezo-actuated high-dynamic compensation mechanism for industrial robots," in *Proc. IEEE/RSJ Int. Conf. on Intelligent Robots and Systems*, San Francisco, CA, USA, September 2011, pp. 4704–4709.

[2] O. Sörnmo, B. Olofsson, U. Schneider, A. Robertsson, and R. Johansson, "Increasing the milling accuracy for industrial robots using a piezo-actuated high-dynamic micro manipulator," in *IEEE/ASME Int. Conf. on Advanced Intelligent Mechatronics*, Kaohsiung, Taiwan, July 2012, pp. 104–110.

[3] A. Puzik, A. Pott, C. Meyer, and A. Verl, "Industrial robots for machining processes in combination with an additional actuation mechanism for error compensation," in *7th Int. Conf. on Manufacturing Research (ICMR)*, University of Warwick, UK, September 2009.

[4] B. Allison and A. Isaksson, "Design and performance of mid-ranging controllers," *J. of Process Control*, vol. 8, no. 5, pp. 469–474, 1998.

[5] A. Sharon, N. Hogan, and D. E. Hardt, "The macro/micro manipulator: An improved architecture for robot control," *Robotics & Computer-Integrated Manufacturing*, vol. 10, no. 3, pp. 209–222, 1993.

[6] B. Allison and S. Ogawa, "Design and tuning of valve position controllers with industrial applications," *Transactions of the Institute of Measurement and Control*, vol. 25, no. 1, pp. 3–16, 2003.

[7] S. Haugwitz, M. Karlsson, S. Velut, and P. Hagander, "Anti-windup in mid-ranging control," in *Proc. 44th IEEE Conf. on Decision and Control and European Control Conf.*, Seville, Spain, Dec. 2005, pp. 7570–7575.

[8] C. Garcia and M. Morari, "Internal model control. a unifying review and some new results," *Industrial & Engineering Chemistry Process Design and Development*, vol. 21, no. 2, pp. 308–323, 1982.

[9] A. Zheng, V. Mayuresh, and M. Morari, "Anti-windup design for internal model control," *Int. J of Control*, vol. 60, no. 5, pp. 1015–1024, 1994.

[10] A. Datta and J. Ochoa, "Adaptive internal model control: design and stability analysis," *Automatica*, vol. 32, no. 2, pp. 261–266, 1996.

[11] G. Silva and A. Datta, "Adaptive internal model control: the discrete-time case," in *Proc. Am. Control Conf.*, vol. 1. San Diego, CA, USA: IEEE, 1999, pp. 547–555.

[12] Q. Hu and G. Rangaiah, "Adaptive internal model control of nonlinear processes," *Chemical Engineering Science*, vol. 54, no. 9, pp. 1205–1220, 1999.

[13] K. Hunt and D. Sbarbaro, "Neural networks for nonlinear internal model control," in *IEE Proc. D of Control Theory and Applications*, vol. 138, no. 5. IET, 1991, pp. 431–438.

[14] S. Gayadeen and W. Heath, "An internal model control approach to mid-ranging control," *IFAC Advanced Control of Chemical Processes*, vol. 7, no. Part 1, pp. 542–547, 2009.

[15] A. Bemporad, "Reference governor for constrained nonlinear systems," *IEEE Trans. on Automatic Control*, vol. 43, no. 3, pp. 415–419, 1998.

[16] E. Gilbert, I. Kolmanovsky, and K. Tan, "Discrete-time reference governors and the nonlinear control of systems with state and control constraints," *Int. J. of Robust and Nonlinear Control*, vol. 5, no. 5, pp. 487–504, 1995.

[17] R. Johansson, *System Modeling and Identification*. Englewood Cliffs, New Jersey: Prentice Hall, 1993.

[18] Heidenhain, 2013, URL: http://www.heidenhain.com.

[19] A. Blomdell, I. Dressler, K. Nilsson, and A. Robertsson, "Flexible application development and high-performance motion control based on external sensing and reconfiguration of ABB industrial robot controllers," in *Proc. Workshop of "Innovative Robot Control Architectures for Demanding (Research) Applications—How to Modify and Enhance Commercial Controllers", IEEE Int. Conf. Robotics and Automation*, Anchorage, AK, USA, June 2010, pp. 62–66.